Prediction of Sea Level Anomalies Using Ocean Circulation Model Forced by Scatterometer Wind and Validation Using TOPEX/Poseidon Data

Yves Quilfen, Abderrahim Bentamy, Pascale Delecluse, Kristina Katsaros, and Nicolas Grima

Abstract—Uncertainties in the surface wind field have long been recognized as a major limitation in the interpretation of results obtained by oceanic circulation models. It is especially true in the tropical oceans, where the response to wind forcing is very strong on short time scales. The purpose of this paper is to show that these uncertainties can be greatly reduced by using spaceborne wind sensors that provide accurate measurements on a global basis.

Surface winds over the global oceans have been measured by scatterometry since the launch of the European Remote Sensing Satellite (ERS-1) in August 1991 by the European Space Agency, Noordwijk, The Netherlands, and is currently provided by ERS-2, launched in April 1995. The ground-track wind vectors are processed to compute mean weekly surface winds onto a 1° square grid at the Institut Francais de Recherche pour l'Exploitation de la Mer (IFREMER), Plouzane, France. These winds are validated by comparison with the buoy array in the tropical Pacific ocean, showing good agreement. In order to further evaluate this wind field, the three-dimensional (3-D) ocean model OPA7 developed at Laboratoire d'Océanographie Dynamique et de Climatologie, Paris, France, is forced over the tropical oceans by the ERS-derived wind stress fields and by fields from the atmospheric model Arpege/Climat. Selected ocean parameters are defined in order to validate the ocean model results with measurements of the tropical ocean and global atmosphere (TOGA) buoys in the Pacific ocean. The ability of the model to describe the short scale (a few weeks to a few years) oceanic variability is greatly enhanced when the satellite-derived surface forcing is used.

In this paper, we present further comparison of the ocean model results with the TOPEX-Poseidon altimeter measurements. Simulated and measured sea level variability are described over the three tropical oceans. The annual and semi-annual signals, as well as the interannual variability, partly linked to the El Niño southern oscillation (ENSO) phenomenon, are well simulated by the OPA7 model when the satellite winds are used. Furthermore, it shows that the objective method, kriging technique, used to interpolate the mean ERS wind fields, dramatically reduces the effects of the satellite bandlike sampling. In the last part of this paper, we focus on the relationship between the wind stress anomalies and the sea level anomalies in the case of the 1997–1998 El Niño event. It clearly shows that sea level anomalies in the eastern and western parts of the Pacific are strongly linked to wind stress anomalies in the central Pacific. The forthcoming scatterometers aboard the METOP and ADEOS satellites will provide a much better coverage. It will enable the wind variability spatial and temporal scales to be resolved better, in order that wind uncertainties no longer blur the interpretation of ocean circulation numerical models results.

Index Terms—Ocean model, ocean surface, scatterometer, sea level.

Manuscript received March 18, 1999; revised December 21, 1999. This work was supported in part by the Programme National de Télédétection Spatiale and in part by the Programme National d'Etude pour la Dynamique du Climat, Paris, France.

Y. Quilfen and A. Bentamy are with the Institut Francais de Recherche pour l'Exploitation de la Mer (IFREMER), Plouzane, France (e-mail: yquilfen@ifremer.fr).

P. Delecluse and N. Grima are with Centre National de la Recherche Scientifique (CNRS), Paris, France.

K. Katsaros is with the Atlantic Oceanographie and Meteorological Laboratories, National Oceanic and Atmospheric Administration (NOAA), Miami, FL 33167 USA.

Publisher Item Identifier S 0196-2892(00)05520-0.

I. Introduction

THE surface wind stress is the main driving force for the ocean but is poorly measured by at-sea instrumentation. Consequently, much attention has been given to the effect of wind uncertainties on the oceanic circulation simulations. Busalacchi *et al.* [1] used a linear model to show that wind uncertainties generate biases in the sea level of the order of or greater than the tropical oceans seasonal and interannual variability. To better interpret the models response, Duchêne and Frankignoul [2] have defined statistical tests to take into account the uncertainties in atmospheric and oceanic data, further demonstrating that the sensitivity to forcing errors is very model-dependent. In addition to the paucity of *in situ* measurements, atmospheric models suffer from uncertainties in various parameterizations affecting the surface wind stress calculation (parameterization of the convection [3] and parameterizations of processes affecting the clouds [4] among others). Frequent changes in these models make the constitution of long-term homogeneous wind data sets for realistic oceanic simulations difficult. Furthermore, the recent atmospheric reanalyzses are not based on the state-of-the-art models and assimilation schemes, and the climate models provide even less realistic simulations.

Recently, Liu *et al.* [5] demonstrated that spaceborne special sensor microwave/imager (SSM/I) winds allow better simulation of the ocean than when using the European Center for Medium-Range Weather Forecast (ECMWF), Reading, U.K., model winds. Nevertheless, SSM/I data also suffer from severe limitations. The wind direction is not currently retrieved from the brightness temperatures, and the estimated surface winds are strongly affected by atmospheric liquid water content at the frequencies used (19 GHz to 85 GHz). The microwave scatterometers (active systems) are spaceborne sensors fully dedicated to surface wind vector measurements and designed to overcome the aforementioned uncertainties: a scatterometer provides global coverage of the ocean with a sufficient resolution for the next system (the NASA/SeaWinds and the

ESA/ASCAT) to resolve the diurnal wind variability, it allows the wind direction to be retrieved accurately. In addition, the wind speed and its signals are not strongly affected by the atmospheric transmission. Freilich and Chelton [6] were the first to demonstrate the ability of scatterometers to retrieve the surface wind spatial and temporal scales of interest for the ocean by using the Ku-band (13.4 GHz) SEASAT scatterometer three months data set described by Jones *et al.* [7]. After this three-month mission in 1978, no scatterometer was flown until the European Space Agency, Noordwijk, The Netherlands, launched the C-band (5.3 GHz) active microwave instrument onboard the ERS-1 satellite in 1991. The ERS-1 scatterometer worked perfectly during nearly five years, and with the ERS-2 satellite having been launched in 1995, these sensors provide a continuous and homogeneous archive of scatterometer winds through the 1990's.

The ERS scatterometers data processed at IFREMER are shown to be highly accurate: about 1.2 m/s and 15° root mean squared error (RMSE) for the wind speed and wind direction, respectively [8], [9], and not significantly affected by rain.

In this paper, we analyze ERS surface wind measurements to examine their adequacy to force the oceanic global circulation model (OGCM) OPA7 [10]. Taking advantage of this wealth of surface wind measurements over a time period covering several annual cycles, mean weekly surface wind and wind stress fields were computed onto a 1° square grid using a statistical interpolation method. This temporal resolution was chosen because the ERS scatterometer coverage is not sufficient to resolve higher scales, but it allows sampling of important features of the tropical atmospheric variability, such as the so-called Madden-Julian oscillations [11] or the wind bursts triggering the oceanic variability in the western Pacific [12], [13]. The 3-D OGCM OPA7 was forced by the ERS winds over the time period 1992-1995, and the results are examined by comparison with the tropical atmosphere and ocean (TAO) buoy array in the Pacific Ocean [14]. To further analyze this experiment, this paper concentrates on the comparison between the simulated sea level and the one measured by the Topex-Poseidon (T/P) altimeter over the three tropical oceans. First, results by Fu and Chao [15] have shown that application of ERS-1 winds results in reduction of the RMSE between the sea level simulated by an oceanic circulation model and measured by the TOPEX/Poseidon altimeter, their analysis concentrating on the mid and high latitudes. In this paper, we intend rather to give a detailed description of the wind patterns and the associated simulated and measured sea level patterns, focusing on the tropical areas, where the response to the wind forcing and to the wind forcing errors are easier to quantify. Indeed, the tropical oceans are mainly wind-driven, and since the ocean response to the wind forcing is faster than in mid-latitudes, it is possible to analyze it over the time period (1992–1997) available for this study.

The data sets are described in Section II. Section III presents a comparison between the scatterometer winds and the TAO winds in three key areas of the tropical Pacific ocean, to assess the adequacy of these different data sources, making measurements at different spatial and temporal scales. In Section IV, we analyze the measured and simulated sea level by means of an empirical orthogonal function (EOF) analysis over the three tropical oceans. We show that the surface topographic structure can be accurately simulated at semi-annual and seasonal time scales. This numerical study is limited to the years 1992–1995, because the heat and freshwater fluxes used to drive the ocean model were not available over a longer time period. Section V then presents an analysis of the T/P sea level and ERS surface wind signals over a longer time period (1993–1997) covering the recent 1997 ENSO event to assess the ability of ERS scatterometers and their follow-on instruments to describe the interannual variability of the surface winds.

II. Data and Model Description

A. Data Description

Two experiments with the OPA7 model, covering the time period 1992–1995, were made concurrently using two different data sets. The first data set consists of the surface fluxes fields (10 m wind-stress vectors, net heat flux, net short-wave radiation flux, and water flux at the sea surface) from the Arpége Climat model (BF5 experiment, Déqué and Piedelièvre [16]). This is a spectral model where measured sea surface temperature (SST) fields [17] are used as a boundary condition.

In the second data set, we used the same solar and water fluxes and the ERS-I wind stress fields. The sensible and latent heat fluxes are computed with bulk formulae, using the Reynolds SST and the ERS-1 scatterometer winds. In computing wind stress from ERS-1, we used the drag coefficients determined by Smith [18]. The computation of ERS-1 scatterometer wind vectors from the radar measurements and their validation are described by Quilfen [19]. The C-band model function CMOD_IFR2 [9] used to compute the wind vector from the radar backscatter measurements is calibrated with the National Data Buoy Center, Stennis Space Center, buoys wind measurements in neutral conditions. The scatterometer wind accuracy estimate is 1.2 m/s and 15° RMS for the wind speed and wind direction, respectively, by comparison with independent NDBC buoy measurements [8], [20]. ERS-1 and ERS-2 were cross-calibrated, and a 0.2 dB bias in ERS-2 measurements was corrected for the time period August 1996 to June 1997. The kriging method used to produce the regular weekly fields is described by Bentamy *et al.* [21]. This interpolating method allows great reduction in the impact of bandlike sampling discussed by Barnier *et al.* [22]. These data are processed and archived by the "Centre ERS d'Archivage et de Traitement" (CERSAT) located at "Institut Français de Recherche pour l'Exploitation de la Mer" (IFREMER).

Wind vectors from the Tropical Atmosphere-Ocean (TAO) buoy array [23], [24] are used to evaluate the ERS-1 winds. To make wind comparisons possible, daily 4-m height wind vectors are referred to 10-m height using the Smith [18] drag coefficient for neutral conditions and are averaged weekly over the same dates as the ERS-1 data.

The sea level anomalies captured by the altimeter TOPEX/POSEIDON (T/P) are used to validate the OGCM responses for the time period 1993/1995. We did not use the 1992 data because they could be affected by calibration errors at the beginning of the T/P mission. We used 10-day, 1° square gridded sea level anomaly heights computed at the University

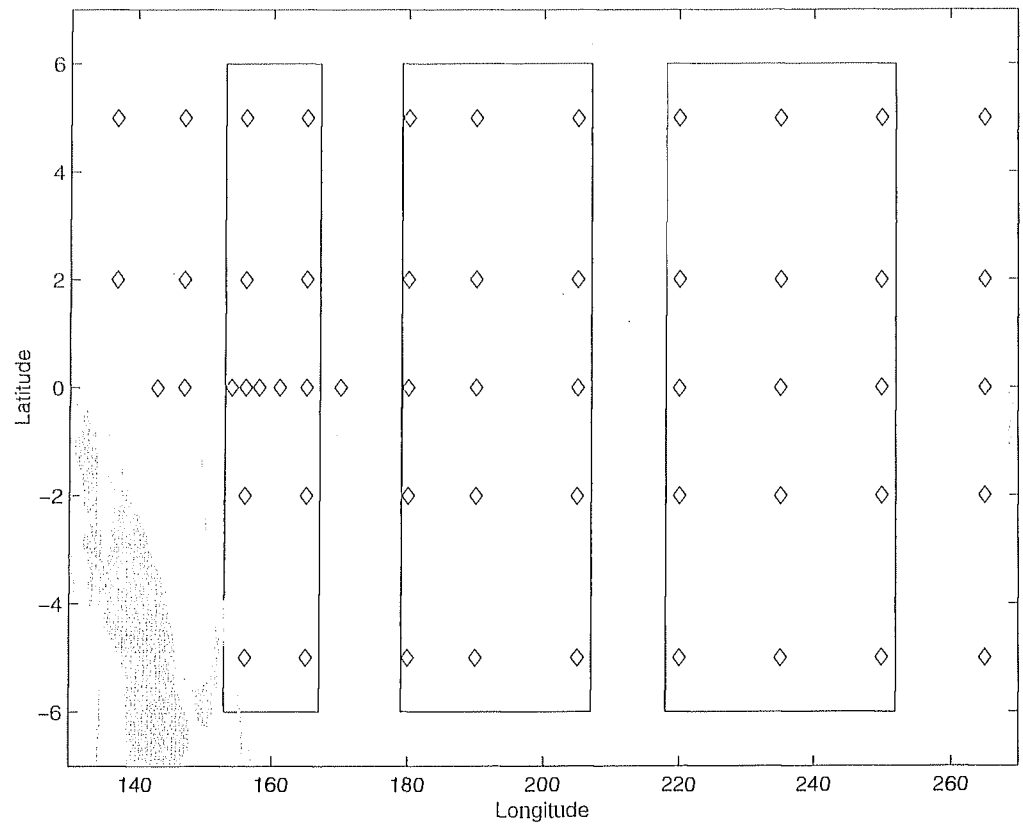

Fig. 1. Positions of the three key areas used to compare ERS and TAO winds. Positions of the TAO buoys are indicated.

of Texas at Austin Center for Space Research (UT/CSR) [25]. The dynamic ocean topography is determined from T/P altimeter data in which all media and instrument corrections (ionosphere, wet and dry troposphere, and electromagnetic bias) and geophysical corrections (tides and inverted barometer) have been applied to the measurements. The altimeter measurements are then reduced to sea surface topography using a precise orbit computed at UT/CSR with the available Satellite Laser Ranging and DORIS doppler tracking data. The altimeter measurements used the precise orbit computed with the JGM-3 Gravity Field model, and an ocean tide correction based on the UT/CSR 3.0 model. Different corrections were additionally applied at UT/CSR to remove oscillator drift and biases in T/P sea level anomalies.

B. Model Description

The OPA7 TOTEM (three tropical oceans version) 3D ocean model developed by modelers from the Laboratoire d'Océanographie DYnamique et de Climatologie [10] was used.

OPA 7 solves the primitive Navier-Stokes equations simplified by the classic hydrostatic and Boussinesq approximations with a rigid lid and incompressibility. An important characteristic of this model is the turbulent kinetic energy (TKE) closure scheme [26] which allows the momentum flux derived from the ERS winds to generate mixing in the upper ocean. Its horizontal domain covers the belt between 50°N and 50°S in latitude and its spatial resolution is irregular. The meridional resolution is 1.5° at the high latitudes and 0.33° at the equator. The zonal resolution in the middle of oceanic basins is 0.75° and 0.33° near coastal regions. The model is defined on 30 vertical levels from 0 to 5000-m with a 10-m resolution in the upper levels. A feedback term constraining the modeled SST toward the observed one is required to prevent excessive surface warming by positive biases in the heat fluxes. We used in this study five-day averaged sea level anomaly computed from the pressure gradient field. The experiment performed with the ERS-1 (Arpége Climat) winds is called ERS/Run (ARP/Run) in the following sections.

III. ERS-1 Scatterometer Winds Assessment

To better interpret the differences between T/P basin-scale sea level anomalies and those simulated by the ERS-1 wind forced ocean model, it is useful to look at how well ERS-1 winds agree with the TAO buoys measurements. To compare the two data sources in a synthetic way, we have defined three key areas of the tropical Pacific: an area in the eastern Pacific containing TAO moorings at 110°W, 125°W and 140°W covering partly the El Niño 3 region; an area in the central Pacific containing TAO moorings at 155°W, 170°W and 180°W covering partly the El Niño 4 region; an area in the western Pacific containing TAO moorings at 154°E, 156°E, 158°E and 165°E covering partly the Warm Pool region (Fig. 1). Weekly ERS-1 and TAO winds were averaged in these areas between 6°N and 6°S. Results are displayed in Figs. 2 and 3 for the zonal and meridional wind components, respectively, for the OPA7 run time period. Correlation coefficients and root mean square differences are

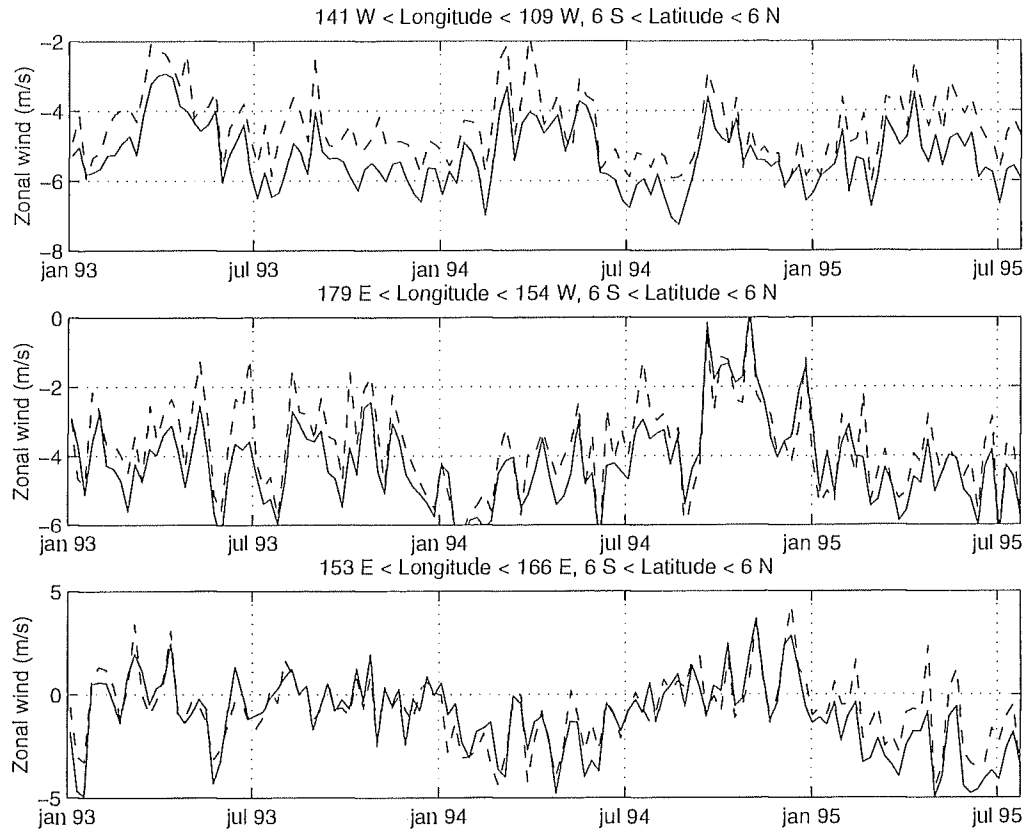

Fig. 2. Weekly averaged zonal wind component (m/s) measured by the TAO buoys (full line) and by the ERS-1 scatterometer (dashed line). The data are further averaged over: El Niño 3 area (top); El Niño 4 area (middle); Warm Pool area (bottom).

indicated in Table I for the El Niño 3, EL Niño 4 and Warm Pool regions. Correlation coefficients are of the order of 0.9 and are significant at the 95% confidence level. The zonal and meridional wind components root mean square differences vary between 0.68 m/s and 0.97 m/s. ERS-1 zonal winds are slightly lower than TAO winds in the eastern Pacific. It is mainly the result of errors in the scatterometer C-band model definition and calibration, which for this example does not take into account the influence of the strong westward south equatorial surface currents in the eastern Pacific ocean [27]. The correlation coefficient is lower and root mean square differences are higher in the western Pacific for the zonal component, partly because the ERS scatterometer sampling is not sufficient to well feature the zonal winds that are highly variable at shorter time scales than in the eastern Pacific. The agreement is nevertheless remarkable for these short-term (a few weeks) fluctuations which represent a large part of the variance signal. The seasonal signal is clearly present in the meridional components while the zonal components exhibit shorter fluctuations, especially in the Warm Pool region in the 30/50 days range of the so-called Madden-Julian oscillations [11]. This region is of special interest because frequent westerly wind bursts are triggering factors for the El Niño events [12], [13].

To summarize, we can say that the ERS scatterometers are able to provide accurate winds to study the basin-scale oceanic circulation in the tropical Pacific with a good resolution and we expect this result to hold in the other oceans.

IV. Sea Level Anomaly Analysis

We intend in this section to provide a global joint view of the sea level anomalies simulated in ERS/Run and measured by T/P. We present also the results obtained by using the Arpège-Climat winds to simulate the SLA (hereafter denoted by ARP/Run SLA) for comparison, although these winds are not very realistic because the Arpège-Climat model does not assimilate any wind observations. Nevertheless this comparison is useful because the atmospheric climate models are currently used for coupled ocean/atmosphere simulations. Validation and improvements of these simulations need better estimates of the surface fluxes as outlined by Delecluse *et al.* [28]. The time period analyzed hereafter covers only 1993/1995, in order to avoid using less accurate T/P measurements at the beginning of its mission.

An efficient way to make the comparisons over the three tropical oceans is to perform an Empirical Orthogonal Function (EOF) analysis of each SLA field and then to compare the significant EOF's. This method splits the field variance into a few significant orthogonal components explaining a high percentage of the total variance, allowing us to describe efficiently the space/time variability patterns [29]. Because the OPA7 experiment only covers two years and a half, it was not possible to separate the annual variability from the interannual one to perform two different EOF analyses. The EOF's were, therefore, computed from the SLA covariance matrix, from which

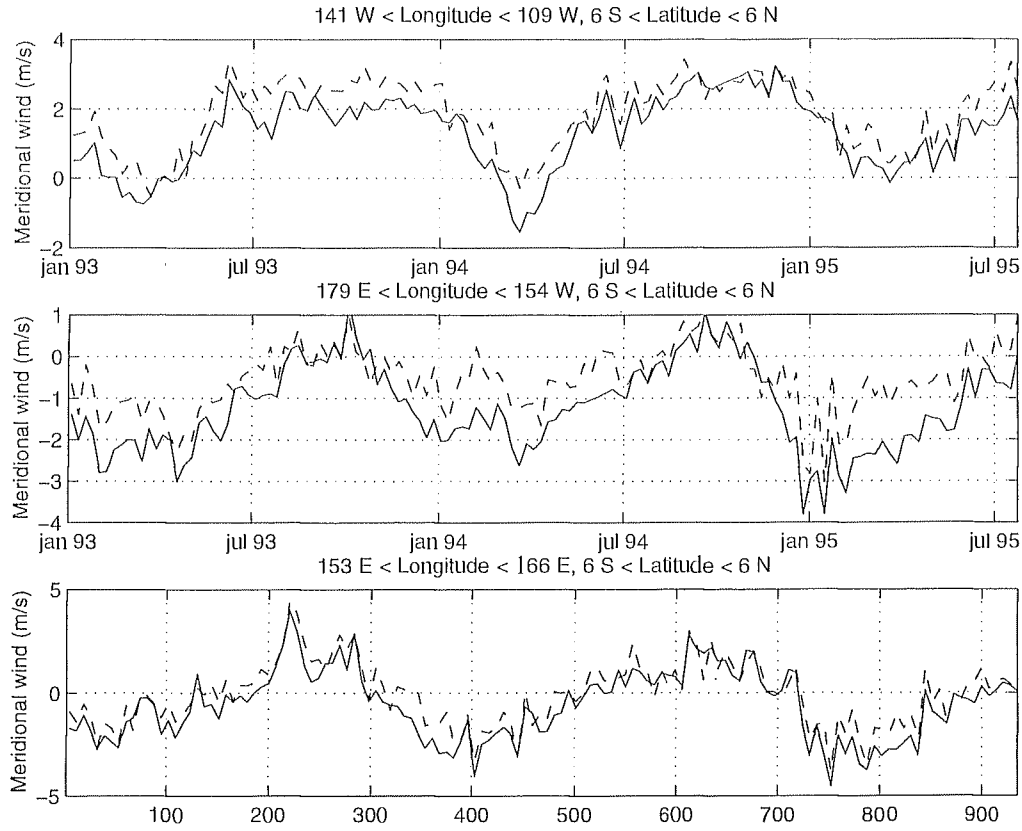

Fig. 3. Weekly averaged meridional wind component (m/s) measured by the TAO buoys (full line) and by the ERS-1 scatterometer (dashed line). The data are further averaged over: El Niño 3 area (top); El Niño 4 area (middle); Warm Pool area (bottom).

TABLE I
CORRELATION COEFFICIENTS AND ROOT MEAN SQUARE DIFFERENCES BETWEEN THE TAO BUOYS AND THE ERS-1 SCATTEROMETER WEEKLY ZONAL AND MERIDIONAL WIND COMPONENTS

Box	El Niño 3	El Niño 4	Warm Pool
U corr.	0.89	0.88	0.86
V corr.	0.93	0.86	0.94
U rms (m/s)	0.91	0.79	0.97
V rms (m/s)	0.68	0.86	0.74

TABLE II
SLA EOF'S OF T/P, ERS/RUN, ARP/RUN (1993–1995)

Mode number	1	2	3	4
T/P variance (&cumul.)	31 (31)	18.5 (49.5)	7.5 (57)	6.4 (63.4)
ERS/Run variance (&cumul.)	26 (26)	24.5 (50.5)	9.6 (60.1)	8 (68.1)
ARP/Run variance (&cumul.)	35 (35)	24 (59)	7.6 (66.6)	5.9 (72.5)
Spat. corr. ERS/Run & T/P	.86	.77	.71	.66
Spat. corr. ARP/Run & T/P	.48	.51	.35	.17
Temp. corr. ERS/Run & T/P	.95	.96	.85	.87
Temp. corr. ARP/Run & T/P	.82	.84	.56	.13

the mean over the experiment duration was substracted, and this analysis will display the interannual modes as well as the annual one. To better support interpretation of these EOF's, we have also computed separately EOF's of the mean annual and interannual T/P SLA signals of the over the five years 1993/1997 (not shown).

The agreement between the measured and the simulated SLA EOF's is measured by computing the correlation coefficients between the EOF's space and time functions. We limit our analysis to the four first components explaining the higher percentages of variance. Indeed, Arnault and Le Provost [30] showed that the components beyond the 4th were likely to be contaminated by residual errors in the CSR3.0 tide model. The components hereafter analyzed are found to be significant following the Overland and Preisendorfer test [31].

A. *EOF's Comparison*

The four first significant EOF's derived for the time period 1993/1995 are described in Table II, their spatial patterns are displayed in Figs. 5 and 6 for T/P and ERS/Run, respectively, and their temporal amplitudes are shown in Fig. 4. ARP/Run results are also indicated in Table II but the EOF's temporal and spatial behaviors are not shown. Indeed, it is worth noting that the climate model Arpège does not assimilate any atmospheric data and is only forced at its low boundary by observed sea surface temperatures. It thus cannot provide an oceanic simulation as realistic as ERS/Run. It is, nevertheless, useful to do the comparison because this atmospheric model is used for coupled experiments with OPA7 and because it well highlights the scatterometer winds impact on the SLA simulation.

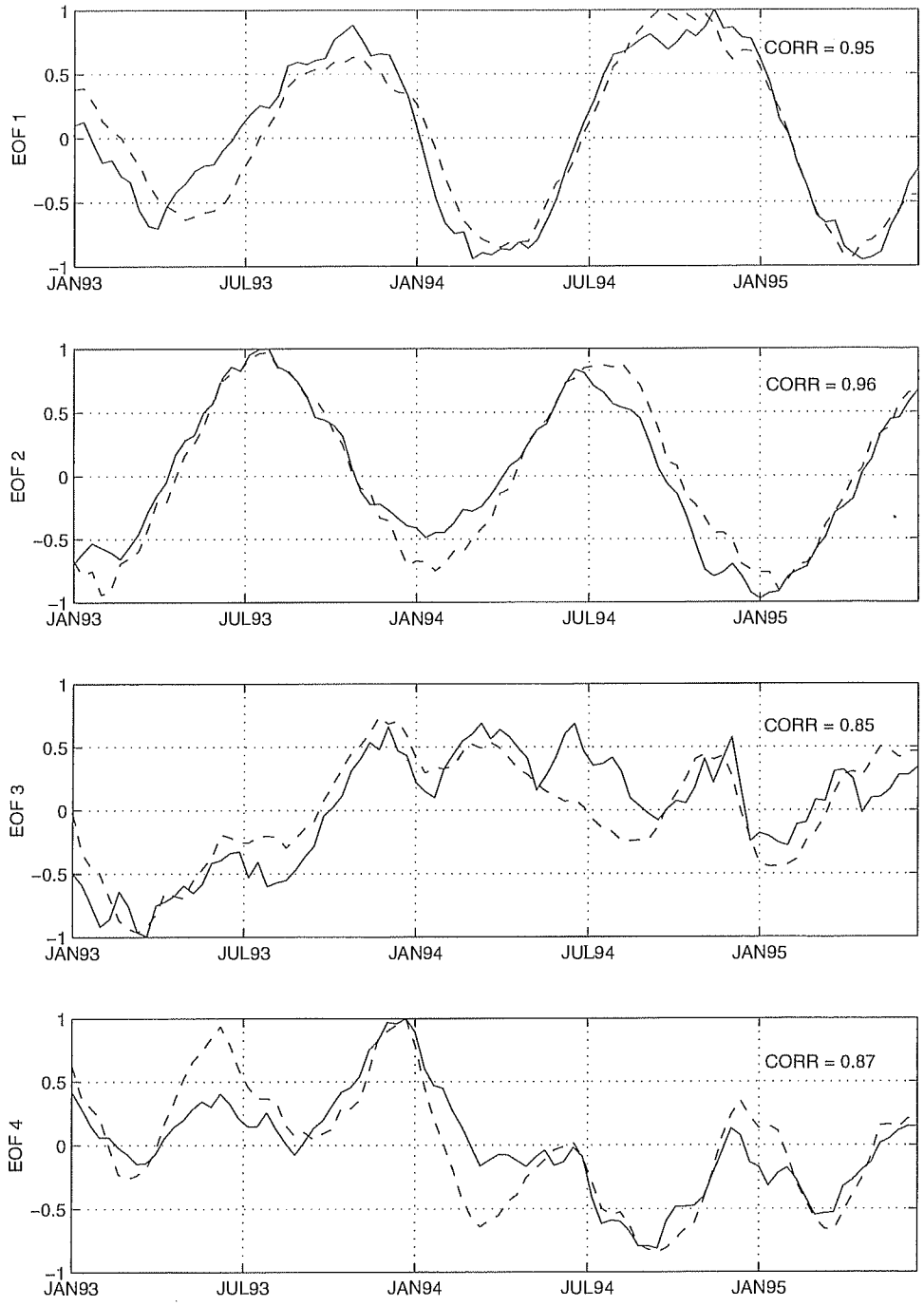

Fig. 4. Time amplitudes of the four first EOF's of T/P SLA (full line) and of ERS/Run SLA (dashed line), from mode 1 (top) to mode 4 (bottom). The series are normalized by their maximum amplitudes. Correlation coefficients are indicated.

The two first EOF's describing together the seasonal SLA variability represent about 50% of the total variance for T/P and ERS/Run and 59% for ARP/Run. There is very little sub-seasonal variability in the Arpege winds, explaining thus a relatively high percentage of variance in the two first ARP/Run EOF's. The lower variance explained by the four first T/P components could be due to the higher mesoscale signals in the measurements compared to the smoother simulated sea level anomalies, although the OGCM grid is finer.

The most interesting result displayed in Table II concerns the correlation level between the measured and the simulated SLA fields. High spatial and temporal correlations are found between T/P and ERS/Run, indicating a very good agreement even for the EOF's 3 and 4 which represent less than 10% of the variance. The agreement between T/P and ARP/Run is generally much lower, except for the temporal part of the annual signal. For both ERS/Run and ARP/Run the spatial correlations are lower than the temporal one, results that can be attributed to real differences in the patterns (Figs. 5 and 6) and to the difference in the T/P and OPA7 grid (simulated SLA were interpolated onto the T/P grid to compute the correlation coefficients).

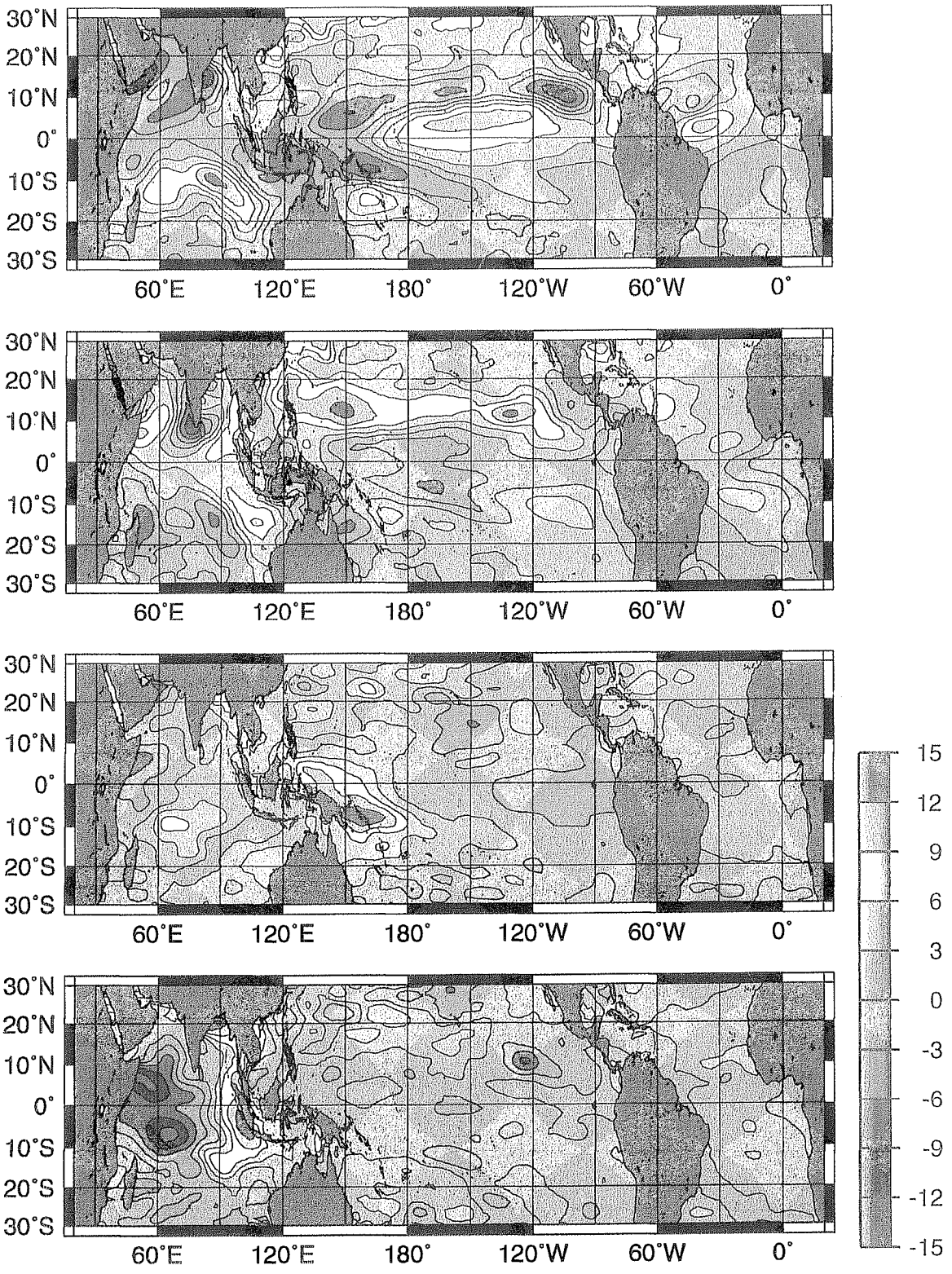

Fig. 5. Spatial amplitudes of the four first EOF's of T/P SLA, from mode 1 (top) to mode 4 (bottom). Units are in centimeters.

In the following section, we analyze and compare the SLA patterns as measured by T/P and as simulated in ERS/Run to further validate the ability of OPA7 forced by ERS-1 scatterometer winds to simulate the main characteristics of the SLA field in the tropical oceans.

B. SLA Characteristic Patterns as Measured by T/P and as Simulated in ERS/Run

The four first SLA EOF's derived for the time period 1993/1995 are displayed in Figs. 5 and 6 for T/P and ERS/Run, respectively. Their temporal modulation is shown in Fig. 4.

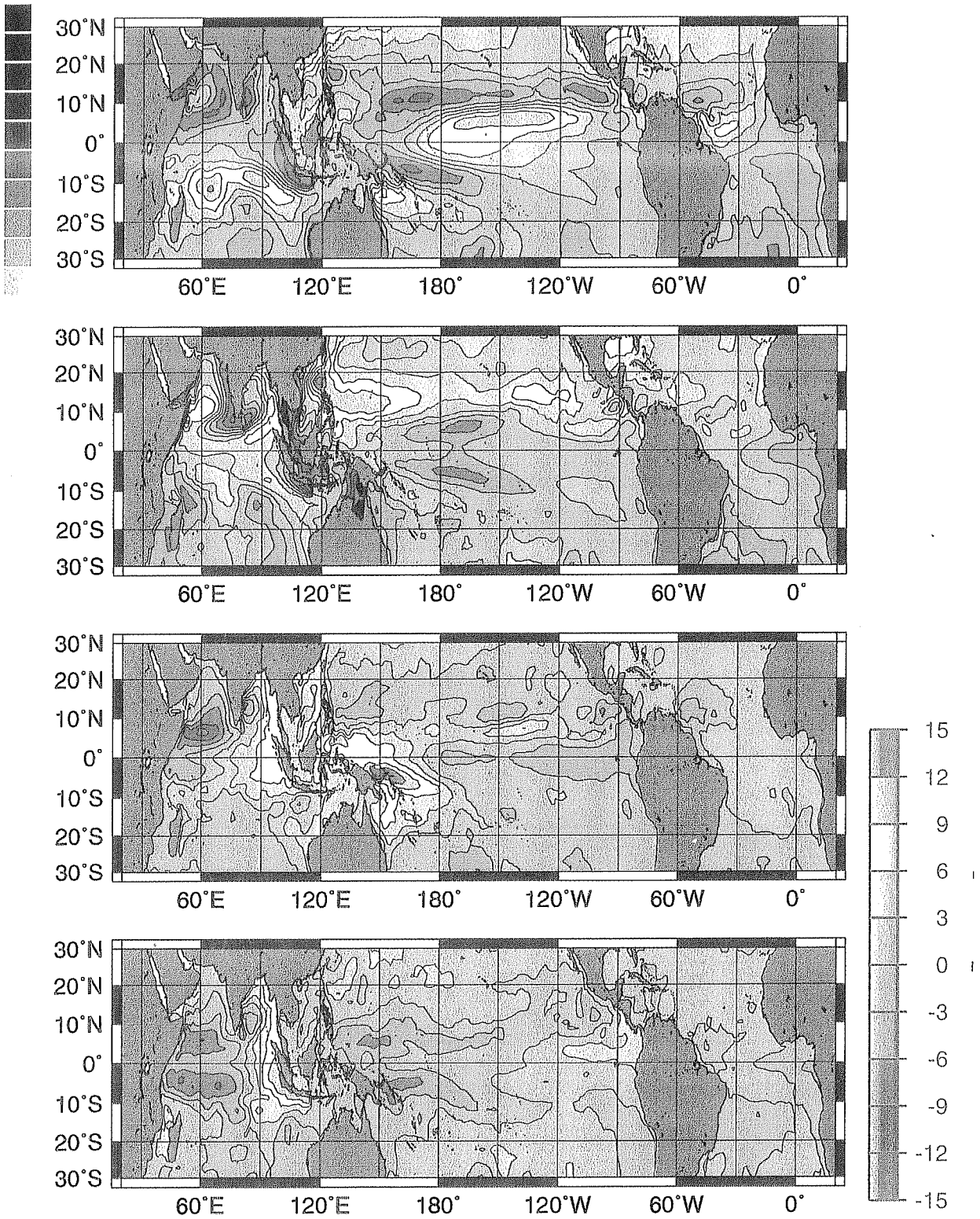

Fig. 6. Spatial amplitudes of the four first EOF's of ERS/Run SLA, from mode 1 (top) to mode 4 (bottom). Units are in centimeters.

They are normalized to express the anomalies directly in centimeters on Figs. 5 and 6.

1) The Annual Variability: The amplitudes of the modes 1 and 2 temporal series describe the annual signal and account for nearly 50% of the total variance for both T/P and ERS/Run fields (Table II). The annual signal is split into two components because the scalar EOF decomposition cannot take into account the propagating features. EOF's 1 and 2 describe, with a phase difference of three months, the strong seasonal variability of the equatorial topographic structure, and a small steric signature with out of phase variability for both hemispheres in EOF 1. This result corroborates the Hendricks *et al.* [32] findings.

Maximum amplitudes greater than 10 cm are located in the northern part of the Pacific and Atlantic oceans, reflecting the shift of the equatorial currents and trade wind systems toward the north during the boreal summer. The sea level varies with a three-month phase difference on both sides of roughly 10°N and varies almost in phase across the Pacific basin. For both T/P and ERS/Run the two first modes in the Pacific and Atlantic oceans explain the sea level seasonal variability linked to the seasonal displacement and variability in strength of the North Equatorial Current and the North Equatorial Countercurrent [32], [33]. In the Indian Ocean the seasonal sea level variability is linked to the seasonal reversal of the ocean circulation following the Asian monsoon. The fact that the seasonal variability is expressed in two components suggests that the SLA's are strongly linked to propagating features as already shown by Périgaud and Delecluse [34], Delcroix *et al.* [35] and Boulanger *et al.* [36]. We are mainly interested in this paper in the comparison between the observed and the modeled sea level anomalies. Table II provides the correlation coefficients between T/P and ERS/Run EOF's. It is 0.95 and 0.96 for the first and second mode temporal amplitudes, respectively, showing the excellent agreement between the simulated and measured SLA's. The spatial correlation for these two modes are 0.86 and 0.77, respectively. It is lower for mode 2, although still significant. Indeed, the main mode 2 SLA patterns are in good agreement but some regional discrepancies appear, such as in the Java Sea and the Gulf of Siam or in the southern part of the Tropical Pacific.

2) *The Semi-Annual and Interannual Variability:* The third mode explains 7.5% and 9.6% of the total variance for T/P and for ERS/Run, respectively. It is predominant in the Pacific ocean. The 4th mode explains 6.4% and 8% of the total variance for T/P and for ERS/Run, respectively. It is predominant in the Indian ocean. Both modes 3 and 4 display a strong zonal oscillation of the sea level with a maximum amplitude of 15 cm. Fig. 4 shows that there is a leakage of higher frequency variability into the interannual one. Due to the short analyzed time period corresponding to the model run (1992/1995), it was not possible to separate the different oscillations. Nevertheless, to verify these EOF's structures, we have also computed the EOF's of the T/P field over the longer time period 1993/1997 (not shown). To do that, we first computed the EOF's of the mean annual cycle, then those of the interannual variability obtained by substracting the mean annual cycle. It appeared that a strong semi-annual cycle occurs at the same location as the interannual variability, explaining the observed leakage in Fig. 4.

Part of mode 3 describes the sea level variability linked to the El Niño/Southern Oscillation phenomenon: negative (positive) SLA's occur in the western (eastern) Pacific during the El Niño phase following a relaxation (increase) of the trade winds, and inversely during the La Nina phase. El Niño's in the 1990s are described in Goddard and Graham [37], (hereafter *GG*). In Figs. 4–6, we observe at the beginning of 1993 negative SLA's in the western Pacific that corresponds to local positive wind stress anomalies [westerly wind bursts, Fig. 2(c)], identified by *GG* as a weak El Niño. It turns then at the beginning of 1994 to a La Nina phase with positive sea level anomalies in the western Pacific that correspond to negative wind stress anomalies in the central Pacific [stronger westerlies, Fig. 2(b)]. *GG* then identified another El Niño warming event at the end of 1994 which is not really readable in the SLA, partly hidden by the strong semi-annual variability, although we observe a trend in the EOF 3 temporal amplitude and westerly wind bursts in the western Pacific [Fig. 2(c)]. This interannual variability is much better delineated when analyzing the signals over the time period 1993–1997 (described in Section V). These 1993–1995 El Niño/La Nina event characteristics were unusual and not well predicted by the forecast models as stated by *GG*. The ability of the OPA7 model forced by scatterometer winds to well simulate these events is, thus, very encouraging. The correlation coefficient between T/P and ERS/Run third EOF's is 0.71 and 0.85 for the spatial and temporal patterns, respectively.

Mode 4 describes a strong zonal oscillation of the sea level between the east and the west part of the Indian Ocean, with negative (positive) SLA's in the west (east) Indian ocean in 1993, and inversely in 1994. We note that for the years 1993 and 1994, the large scale anomalies in the western and eastern part of the Pacific and Indian oceans are of the same sign, with a phase shift hardly computable over this short time period. A characteristic feature appearing in Figs. 5 and 6 is the twin pattern on both sides of the equator in the western Indian ocean. This mode is very different from the one described by Hendricks *et al.* [32], probably due to the fact that his analysis extended up to 60° of latitude. One more time we observe a good agreement between the ERS/Run and T/P signals, the correlation coefficients being 0.66 and 0.87 for the spatial and temporal patterns, respectively.

A characteristic feature of this EOF analysis is the relatively low amount of interannual variability in the Atlantic Ocean compared with the Pacific and Indian Oceans.

This EOF analysis also shows that the objective method, kriging technique, used to interpolate the mean ERS wind fields reduces dramatically the effects of the satellite bandlike sampling, since we have not evidenced any related pattern in the EOF's.

To summarize this section, we have shown that these winds can be used to produce a realistic numerical simulation of the annual and interannual sea level variability. Moreover, the global coverage of the ERS scatterometers, of the T/P altimeter, and of the OPA7 model allow the analysis to address the ocean–atmosphere interactions at global scale as well as at basin scale. The agreement between the simulated and measured SLA's further shows that the errors in the three components of this system are low enough to generate confidence in both observed and simulated SLA and geostrophic currents.

To further illustrate such a conclusion, we analyze in the following section the surface wind forcing by ERS-1 and 2 scatterometers and the sea level response as measured by T/P over the five years 1993–1997. This time period includes the 1997 El Niño event, providing a good opportunity to analyze the scatterometer signal for that extreme case.

V. Surface Winds and SLA in the Tropical Pacific Ocean (1993–1997)

We intend in this section to give a brief description of the surface winds and sea level anomalies in the tropical Pacific Ocean during the years 1993 through 1997 to illustrate the ability of

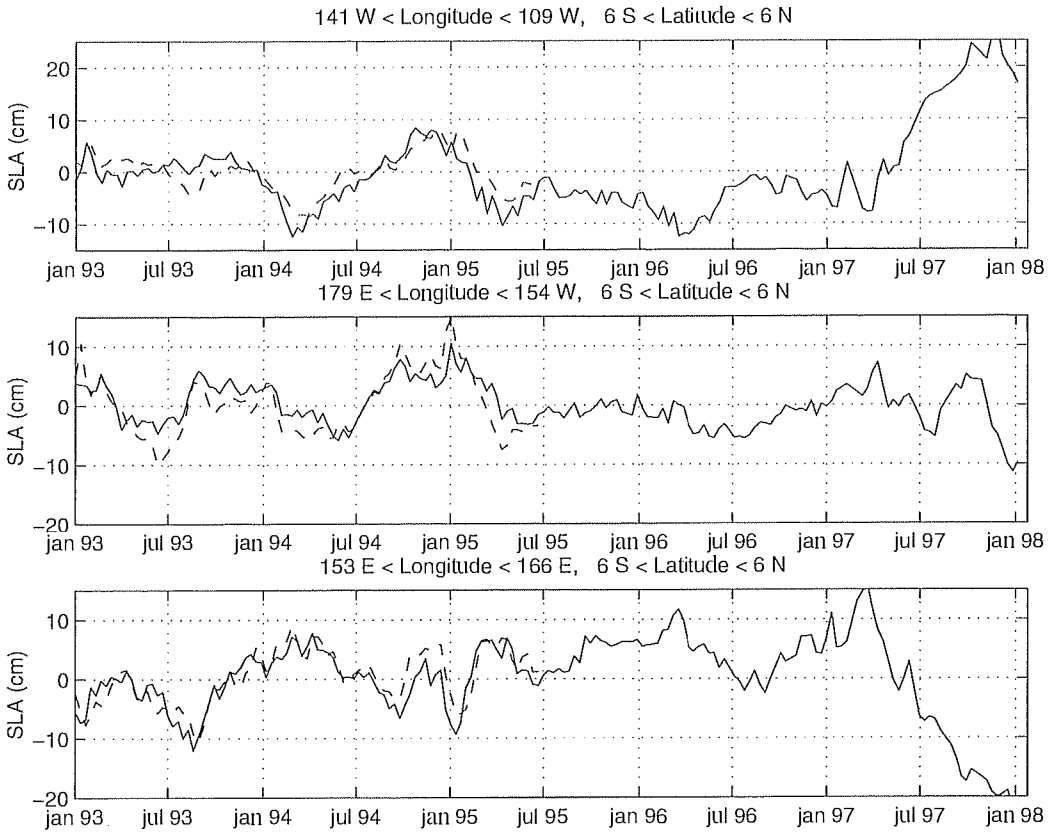

Fig. 7. Mean ten-day averaged sea level anomalies measured by the T/P altimeter (full line over the time period 1993/1997) and simulated in the ERS/Run run (dashed line over the time period January 1993 to July 1995). The data are further averaged over (top) El Niño 3 area; (middle) El Niño 4 area; (bottom) Warm Pool area.

this scatterometer data source to feature the main wind patterns for studying the ocean variability. The scatterometer data used in this section include both the ERS-1 and ERS-2 measurements, and the T/P data are used from cycle 11 through cycle 195.

Fig. 7 displays, for the three areas defined in Section III, the SLA measured by T/P over the time period 1993–1997 and simulated in ERS/Run over the time period January 1993–July 1995 for comparison purpose. Fig. 8 displays, for the same areas, the zonal wind component measured by the ERS-1 and 2 scatterometers over the time period 1993 through 1997.

The beginning of the analyzed time period is characterized by a persistent weak warming across the equatorial Pacific, in continuation with the 1992 El Niño event. A deeper thermocline is observed, the anomalies propagating from west to east from the end of 1992 to the beginning of 1993 [37], [14]. It is accompanied by negative SLA (lower sea level) and westerly wind bursts in the western Pacific, as shown in Figs. 7(c) and 8(c), respectively. Sea surface temperatures then return to near normal at the end of 1993 and the beginning of 1994. It is accompanied by an increase (lowering) of the sea level in the western (eastern) Pacific. The second half of 1994 is characterized by another surface warming and a deeper thermocline east of the dateline. The sea level is higher in that region and lower in the western Pacific, characteristic features of El Niño events. During this period, we observe a weakening of the zonal winds in the central Pacific and strong westerly wind bursts in the western Pacific. Although the mechanisms inducing these warmings are quite different [37], [38] and not completely understood, and despite a quite weak signal, we observe a remarkable agreement over the time period 1993 through 1995 between the measured and simulated SLA (Fig. 7). It further demonstrates, together with results of Section III, that the scatterometers are able to measure the wind variability associated with these warming events. Both 1993 and 1994 warmings were associated with westerly anomalies in the western Pacific and to a lesser extent in the central Pacific. The situation then has shifted to a La Nina phase in 1995 and 1996, with lower SST's across the Pacific, higher (lower) sea level in the western (eastern) Pacific, and prevailing easterlies across the entire basin. The 1997-1998 El Niño event is the strongest that has developed in the past decades. We indeed observe on Fig. 8 very strong westerly wind bursts at the beginning of 1997 in the western Pacific, conditions that prevailed throughout the year. In the central Pacific, we observe a decrease in the easterlies that become westerlies in the second half of the year, translating the convective regions toward the east. Wind anomalies in the eastern part of the basin are not spectacular, remaining within the observed annual amplitudes. The wind anomalies in the central and western Pacific correspond to a dramatic change in the sea level in the eastern and western Pacific. SLA in the eastern and western Pacific, as well as westerly wind anomalies in the central Pacific, are several times greater than those corresponding to the 1993 and 1994 warmings, reflecting the amplitude of this El Niño event. The remarkable feature is the phase variability between the zonal wind

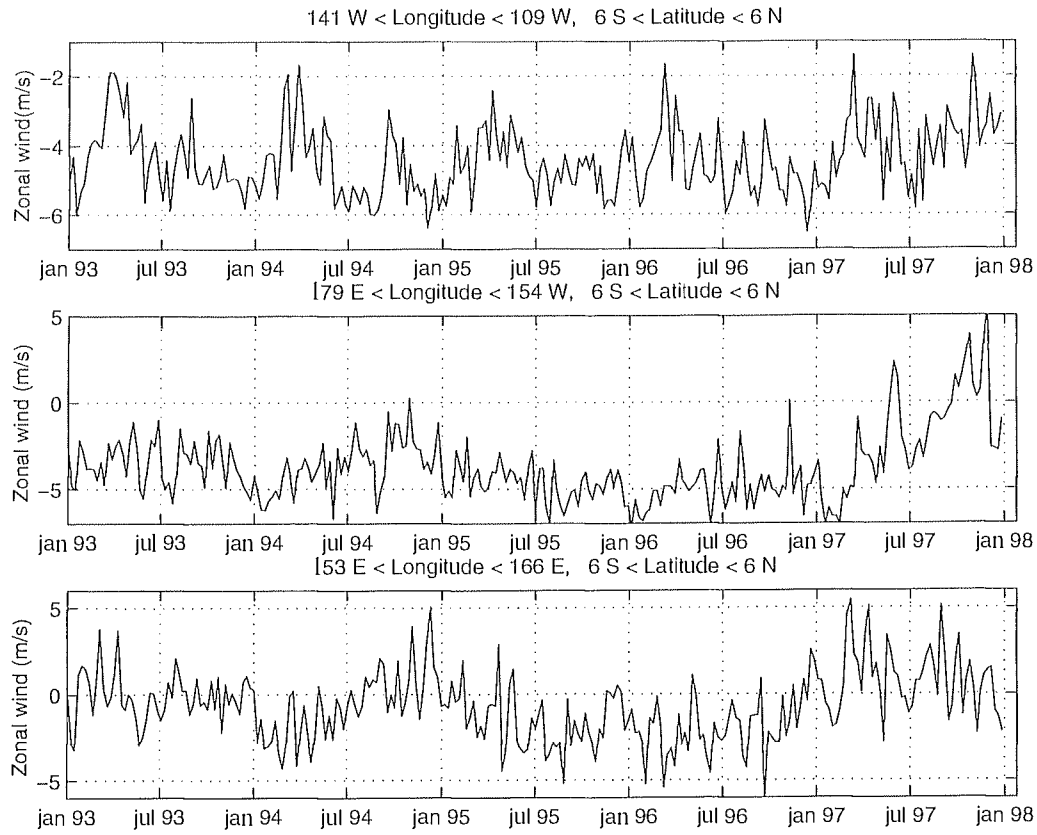

Fig. 8. Weekly averaged zonal wind component (m/s) measured by the ERS-1 and ERS-2 scatterometers. The data are further averaged over: (top) El Niño 3 area; (middle) El Niño 4 area; (bottom) Warm Pool area.

stress anomalies in the central part of the Pacific [Fig. 8(b)] and the sea level anomalies in the eastern and western parts [Fig. 7(a) and (c)].The maximum correlation is 0.92 and −0.94, respectively, when the wind anomalies lead the SLA by 20 days. These results are obtained after interpolating the winds to the sea level measurement dates and after applying a 140-day median filter to both time series in order to remove the short-term fluctuations. During the 1997-1998 El Niño, strong westerly anomalies in the central Pacific are associated with strong SLA in the western and eastern parts of the Pacific, as already noted for the precedent El Niño's [37].

The results of this section qualitatively and quantitatively assess the adequacy of scatterometer measurements for large scale oceanic studies. This will lead to investigation of the annual and interannual ocean variability mechanisms in the tropical oceans by using the scatterometer wind data over long time periods, jointly with all other observational means and modeling tools.

VI. Conclusion

The aim of this paper is to demonstrate the adequacy of spaceborne scatterometers to provide accurate wind stress fields for oceanic studies. A homogeneous archive of such data covering several years is now available from the ERS-1 and 2 scatterometers. These data were validated through comparisons with various other data sets derived from *in situ* measurements or from atmospheric models [21], [8], [20] and also in the context of a geophysical study [14], [9]. We focus here on the large-scale sea level variability in the tropical oceans, which has the characteristic that it reacts strongly and quickly to the atmosphere's variability, allowing the study of the impact of scatterometer winds. Moreover, the limited coverage by the ERS scatterometer is sufficient for capturing most of the tropical atmosphere variability at scales of interest for the oceanic circulation. Thus, the sampling problems that occur at higher latitudes do not apply as severely in the tropics. We show in this paper that the weekly scatterometer winds very well correlate with the TAO buoy winds with correlation coefficients as high as 0.9 in three areas of the tropical Pacific covering the TAO array.The zonal and meridional wind components standard deviations vary between 0.9 m/s and 1.6 m/s. The agreement is better in the central and eastern Pacific and lower in the Warm Pool area where the wind variability is greater. In this latter area, the scatterometer nevertheless clearly features the wind variability at the time scale of a few weeks, including the so-called Madden-Julian oscillations and the westerly wind bursts that are important triggering factors for the ocean [12], [13].

To go beyond this validation, the OGCM OPA7 has been forced with scatterometer derived momentum fluxes, with bulk sensible and latent heat fluxes computed with scatterometer winds and observed SST's, and with precipitation and solar fluxes from an atmospheric climate model over the time period of 1992–1995 (run ERS/Run). A concurrent run has also been performed by using only fluxes from the atmospheric model (run ARP/Run). An EOF analysis of the simulated sea level and of the T/P measurements is used to test the numerical

model results with the objective of wind validation. Four significant EOF's are identified to describe the large-scale geophysical variability. They account for the sea level seasonal variability in the three tropical oceans, and for the semi-annual and interannual signals in the Indian and Pacific oceans. The variability at scales different from the seasonal one is partly hidden in the Atlantic ocean by the strong signals in the other oceans and thus should be investigated in a separate analysis. The poor correlation between T/P and ARP/Run emphasizes the weaknesses of the atmospheric climate model to reproduce realistic winds. Unrealistic spatial patterns of the sea level are produced in ARP/Run, which fails also to reproduce the annual and semi-annual signals. On the other hand, the comparison between T/P and ERS/Run emphasizes the accuracy of ERS-1 scatterometer winds. Correlation coefficients between the EOF's spatial and temporal patterns are highly significant, although the spatial ones are lower because of the difference in the model and T/P grid and structures. The model resolution is higher and thus, the sea level patterns are also finer. The sea level anomalies are of the same order in the simulated and measured fields, rising to 15 cm in the Pacific and Indian oceans. The seasonal variability of the topographic ridges depicted by the two first modes are in agreement in the three oceans. It depicts mainly the seasonal reversal of the circulation in the Indian Ocean following the extension of the northward (southward) winds during the monsoon onset (breakdown) and the seasonal variability of the North Equatorial Current and Countercurrent in the Atlantic and Pacific oceans. The agreement is excellent everywhere except at a few locations such as the Java Sea, where many factors could explain the discrepancy.

Modes 3 and 4 describe the semi-annual and interannual variability in the Pacific and Indian oceans, respectively. They both feature zonal oscillations of the sea level between the east and west parts of the basins with amplitudes as high as 15 cm. The connection between the two basins is hardly discernible giving the short analyzed time period. Mode 3 features the zonal seesaw in the sea level linked to the El Niño events. The correlation coefficients between the T/P and ERS/Run temporal and spatial patterns are 0.85 and 0.71, respectively. Note that an analysis restricted to the Pacific Ocean would have increased this latter correlation. The Indian ocean has also experienced a large interannual zonal oscillation during this time period, as shown in mode 4.

The EOF analysis has shown the very good agreement between the simulated and the measured sea level, even for the higher-order significant modes. It thus assesses the scatterometer wind accuracy for the large-scale ocean circulation studies. In the last section, we have described the wind and sea level variability over a longer time period (1993 through 1997) in order to cover the recent 1997–1998 El Niño event. The amplitude of this event is reflected in the wind and sea level, which present large anomalies. We observe at the beginning of 1997 strong westerly wind bursts in the western Pacific that occur throughout the year. We observe also at the beginning of 1997 a significant weakening of the trade winds in the central Pacific near the date line, and they reverse, for the first time during 1993 through 1997, to westerly winds in the second half of 1997. As warm water and convective activity are displaced toward the east, we also observe an increase in the meridional winds toward the equator. The wind anomalies produce a drastic lowering of the zonal sea level gradient. We observe negative and positive sea level anomalies of 20 cm amplitude in the western and eastern Pacific, respectively.

In summary, we have shown that the scatterometer winds allow accurate simulation of the annual and interannual sea level variability with a realistic 3-D model in the tropics. Moreover, the global coverage of the ERS scatterometers with suitable resolution of the T/P altimeter and of the OPA7 model allow the analysis of the ocean–atmosphere interactions at a global scale as well as at a basin scale. The agreement between the simulated and measured sea level anomalies further shows that the errors in the three components of this system are low enough to give confidence in both observed and simulated SLA's and geostrophic currents. One of the Seawinds U.S. scatterometers is already in orbit aboard the QuikScat satellite, and the forthcoming ASCAT European scatterometers will insure a better and longer coverage to extend the application of scatterometer winds.

ACKNOWLEDGMENT

The authors wish to thank the Centre ERS d'Archivage et de Traitement, Plouzane, France, D. Chambers and M. J. McPhaden for providing the ERS scatterometer, the T/P altimeter, and the TAO buoy data, respectively, and C. Levy for her help with the OPA7 model. They would also like to thank Y. Du Penhoat for helpful comments. Allocation of computer time on Cray2 for running the ocean model has been provided by the Institut de Developpement et des Ressources en Informatique Scientifique (IDRIS), Orsay, France.

REFERENCES

[1] A. J. Busalacchi, M. J. McPhaden, J. Picaut, and S. R. Springer, "Sensitivity of wind-driven tropical Pacific Ocean simulations on seasonal and interannual time scales," *J. Marine Syst.*, vol. 1, pp. 119–154, 1990.

[2] C. Duchêne and C. Frankignoul, "Seasonal variations of surface dynamic topography in the Tropical Atlantic: Observational uncertainties and model testing," *J. Marine Syst.*, vol. 2, pp. 223–247, 1991.

[3] M. J. Miller, C. M. Beljaars, and T. Palmer, "The sensitivity of the ECMWF model to the parameterization of evaporation from the tropical oceans," *J. Climate*, vol. 5, pp. 418–434, 1992.

[4] J. M. Slingo, K. R. Sperber, J. S. Boyle, J.-P. Ceron, M. Dix, B. Dugas, W. Ebisuzaki, J. Fyfe, D. Gregory, J.-F. Gueremy, J. Hack, A. Harzallah, P. Inness, A. Kitoh, W. K.-M. Lau, B. McAvaney, R. Madden, A. Matthewa, T. N. Palmer, C.-K. Park, D. Randall, and N. Renno, "Intraseasonal oscillations in 15 atmospheric general circulation models: Results from an AMIP diagnostic subproject," *Clim. Dynam.*, vol. 12, pp. 325–357, 1995.

[5] W. T. Liu, W. Tang, and R. Atlas, "Responses of the tropical pacific to wind forcing as observed by spaceborn sensors and simulated by an ocean general circulation model," *J. Geophys. Res.*, vol. 101, pp. 16 345–16 359, 1996.

[6] M. H. Freilich and D. B. Chelton, "Wavenumber spectra of pacific winds measured by the Seasat scatterometer," *J. Phys. Oceanog.*, vol. 16, pp. 741–757, 1986.

[7] W. L. Jones, L. C. Schroeder, D. H. Boggs, E. M. Bracalente, R. A. Brown, G. J. Dome, W. J. Pierson, and F. J. Wentz, "The seasat—A satellite scatterometer: The geophysical evaluation of remotely sensed wind vectors over the ocean," *J. Geophys. Res.*, vol. 87, pp. 3297–3317, 1982.

[8] H. C. Graber, N. Ebuchi, and R. Vakkayil, "Evaluation of ERS-1 Scatterometer Winds with Wind and Wave Ocean Buoy Observations," Tech. Rep. RSMAS 96-003, Rosentiel School Marine Atmos. Sci., Univ. Florida, Miami, FL, 1996.

[9] Y. Quilfen, B. Chapron, T. Elfouhaily, K. Katsaros, and J. Tournadre, "Observation of tropical cyclones by high resolution scatterometry," *J. Geophys. Res.*, vol. 104, pp. 7967–7989, Apr. 1998.

[10] P. Delecluse, G. Madec, M. Imbard, and C. Levy, "Int. Rep. LODYC 93/05," OPA Version 7 Ocean General Circulation Model Reference Manual, 1993.

[11] R. A. Madden and P. R. Julian, "Observations of the 40–50-day tropical oscillation—A review," *Mon. Weather Rev.*, vol. 122, pp. 814–837, 1993.

[12] T. Delcroix, G. Eldin, M. McPhaden, and A. Morlière, "Effects of westerly wind bursts upon the western equatorial Pacific Ocean," *J. Geophys. Res.*, vol. 98, pp. 16 379–16 385, 1993.

[13] C. Maes, P. Delecluse, and G. Madec, "Impact of westerly wind bursts on the warm pool of the TOGA-COARE domain in an OGCM," *Clim. Dynam.*, vol. 14, pp. 55–70, 1998.

[14] N. Grima, A. Bentamy, P. Delecluse, K. Katsaros, C. Levy, and Y. Quilfen, "Sensitivity of an oceanic general circulation model forced by satellite wind stress fields," *J. Geophys. Res.*, vol. 104, pp. 7967–7989, 1998.

[15] L. L. Fu and Y. Chao, "The sensitivity of a global ocean model to wind forcing: A test using sea level and wind observations from satellites and operational wind analysis," *Geophys. Res. Lett.*, vol. 24, pp. 1783–1786, 1997.

[16] M. Déqué and A. Piedelièvre, "High resolution climate simulation over Europe," *Clim. Dynam.*, vol. 11, pp. 321–339, 1995.

[17] R. W. Reynolds, "A real-time global sea surface temperature analysis," *J. Climate*, vol. 1, pp. 75–86, 1988.

[18] S. D. Smith, "Coefficients for sea surface wind stress, heat flux, and wind profiles as a function of wind speed and temperature," *J. Geophys. Res.*, vol. 93, pp. 15 467–15 472, 1988.

[19] Y. Quilfen, "ERS-1 Off-Line Wind Scatterometer Products,", Paris, France, Tech. Rep., Inst. Français Rec. l'Exploitation MER/CERSAT, 1995.

[20] Y. Quilfen, B. Chapron, A. Bentamy, J. Gourrion, T. Elfouhaily, and D. Vandemark, "Global ERS-1/2 and NSCAT observations: Upwind/crosswind and upwind/downwind measurements," *J. Geophys. Res.*, vol. 104, pp. 11 459–11 469, May 1999.

[21] A. Bentamy, Y. Quilfen, F. Gohin, N. Grima, M. Lenaour, and J. Servain, "Determination and validation of average wind field from ERS-1 scatterometer measurements," *Global Atmos. Ocean Syst.*, vol. 4, pp. 1–29, 1996.

[22] B. Barnier, J. C. Capella, and J. J. O'Brien, "The use of satellite scatterometer winds to drive a primitive equation model of the Indian Ocean: The impact of bandlike sampling," *J. Geophys. Res.*, vol. 99, pp. 14 187–14 196, 1994.

[23] S. P. Hayes, L. J. Mangum, J. Picaut, A. Sumi, and K. Takeuchi, "TOGA-TAO: A moored array for real-time measurements in the tropical Pacific Ocean," *Bull. Amer. Meteorol. Soc.*, vol. 72, pp. 339–347, 1991.

[24] M. J. McPhaden and S. P. Hayes, "On the variability of winds, sea surface temperature, and surface layer heat content in the western equatorial pacific," *J. Geophys. Res.*, vol. 96, pp. 3331–3342, 1991.

[25] B. D. Tapley, D. P. Chambers, C. K. Shum, R. J. Eanes, and J. C. Ries, "Accuracy assessment of the large-scale dynamic ocean topography from TOPEX/POSEIDON altimetry," *J. Geophys. Res.*, vol. 99, pp. 24 605–24 617, 1994.

[26] B. Blanke and P. Delecluse, "Variability of the tropical Atlantic ocean simulated by a general circulation model with two different mixed-layer physics," *J. Phys. Oceanog.*, vol. 23, pp. 1363–1388, 1993.

[27] Y. Quilfen, A. Bentamy, B. Chapron, T. E. Fouhaily, J. Gourrion, and D. Vandemark, "On the differing response of Ku- and C-band scatterometers," in *Proc. ADEOS & ADEOS-II Symp.*, Kyoto, Japan, Dec. 6–10, 1999.

[28] P. Delecluse, M. Davey, Y. Kitamura, S. G. H. Philander, M. Suarez, and L. Bengtsson, "TOGA review paper: Coupled general circulation modeling of the tropical pacific," *J. Geophys. Res.*, vol. 103, pp. 14 357–14 373, 1998.

[29] R. E. Davis, "Predictability of sea surface temperature and sea level pressure anomalies over the North Pacific Ocean," *J. Phys. Oceanog.*, vol. 6, pp. 249–266, 1976.

[30] S. Arnault and C. L. Provost, "Regional identification in the tropical Atlantic Ocean of residual tide errors from an empirical orthogonal function analysis of TOPEX/POSEIDON altimetric data," *J. Geophys. Res.*, vol. 102, pp. 21 011–21 036, 1997.

[31] J. E. Overland and R. W. Preisendorfer, "A significance test for principal components applied to a cyclone climatology," *Mon. Weather Rev.*, vol. 110, pp. 1–4, 1982.

[32] J. R. Hendricks, R. R. Leben, G. H. Born, and C. J. Koblinsky, "Empirical orthogonal function analysis of global TOPEX/POSEIDON altimeter data and implications for detection of global sea level rise," *J. Geophys. Res.*, vol. 101, pp. 14 131–14 145, 1996.

[33] S. Arnault and R. E. Cheney, "Tropical Atlantic sea level variability from Geosat (1985–1989)," *J. Geophys. Res.*, vol. 99, pp. 18 207–18 223, 1994.

[34] C. Périgaud and P. Delecluse, "Annual cycle in the tropical Indian Ocean," *J. Geophys. Res.*, vol. 97, pp. 20 169–20 178, 1992.

[35] T. Delcroix, J. P. Boulanger, F. Masia, and C. Menkes, "Geosat-derived sea level and surface current anomalies in the equatorial Pacific during the 1986–1989 El Niño and La Nina," *J. Geophys. Res.*, vol. 99, pp. 25 093–25 107, 1994.

[36] J. P. Boulanger, P. Delecluse, C. Maes, and C. Levy, "Long equatorial waves in a high-resolution OGCM simulation of the tropical Pacific Ocean during the 1985–94 TOGA period," *Mon. Weather Rev.*, vol. 125, pp. 972–984, 1997.

[37] L. Goddard and N. E. Graham, "El Niño in the 1990s," *J. Geophys. Res.*, vol. 102, pp. 10 423–10 436, 1997.

[38] G. T. Mitchum, "Trade winds fluctuations associated with El-Niño southern oscillation events," *J. Geophys. Res.*, vol. 92, pp. 9464–9468, 1987.

Yves Quilfen received the Ph.D. degree in 1985 from the University of Paris VI, Paris, France, focusing his research on "the interannual variability of the ocean-atmosphere system in the tropical Atlantic ocean."

From 1986 to 1991, he was with Compagnie de Recherche et d' Etudes Oceanographiques, (CREO), La Rochelle, France, working on defining the ERS-1 scatterometer algorithms. As a Scatterometer Project Scientist with the Institut Francais de Recherche pour l'Exploitation de la Mer (IFREMER) since 1991, he is in charge of the scientific works on the products delivered by IFREMER. Since 1994, he has been primarily involved in the use of satellite microwave measurements for tropical cyclone studies and air–sea fluxes for the ocean circulation.

Abderrahim Bentamy received the Ph.D. degree in numerical analysis and fluid mechanics in 1986 from the Institut National des Sciences Appliquées de Rennes (INSA), Paris, France, for his numerical and theorical studies on Newtonian fluid modeling.

He is currently with the Institut Français de Recherche pour l'Exploitation de la MER (IFREMER), where he has worked on the calibration and validation of ERS-1 scatterometer. This has included a buoy network buoy design used to validate remotely sensed winds, located in Brittany sea (TOSCANE experiment) and Norwegian sea (RENE-91 experiment). He has studied and developed a C-band model relating backscatter coefficient (measured by scatterometer) to surface wind vectors. The latter is routinely used to estimate scatterometer off-line wind products. He is also involved in NSCAT and Quik-Seat scatterometer projects as a Principal Investigator. He is currently investigating the estimation of surface fluxes using and combining active and passive data for ocean studies and especially for ocean circulation forcing.

Pascale Delecluse is the Directeur de Recherche with CNRS. She is attached to the Laboratoire d'Océanographie Dynamique et de Climatologie—Unité Mixte de Recherche CNRS/UPMC/IRD, Centre National de la Recherche Scientifique (CNRS), Paris France, since 1987. Her laboratory is part of the Institut Pierre Simon Laplace, Paris France, where she is in charge, with Hervé Le Treut, of the modeling Pole. She works on the tropical ocean physics and on the development of parameterizations to improve the simulation of the ocean (vertical mixing, mixed layer, barrier layer, etc.) and participates in the development and interpretation of the coupled general circulation models. She is also Chairman of the Programme National d'Etude de la Dynamique du Climat.

Kristina Katsaros was born in Goteborg, Sweden. She received the Dipl. Phys. and Ph.D. degrees from the University of Washington, Seattle.

Until 1990, she was a Research Associate, Research Assistant Professor, Research Associate Professor and Professor, respectively, with the University of Washington, and from 1990 to 1996, she was a Professor with the same university. From 1992 to 1996, she was the Director of the Département d'Océanographie Spatiale, Institut Français de Recherche pour l'Exploitation de la MER (IFREMER). Since 1997, she has been the Director of the Atlantic Oceanographie and Meteorological Laboratories, National Oceanic and Atmospheric Administration (NOAA), Miami, FL.

Nicolas Grima received the Ph.D. degree from the University of Paris VII, Paris, France, in 1988, where he worked on the calculation of gridded wind and wind stress fields from the ERS scatterometer and on the evaluation of these fields for ocean numerical modeling.

In 1998, he worked on the development of a high resolution ocean model. He is currently with the Institut de Developpement et des Ressources en Informatique Scientifique (IDRIS), Orsay, France. Laboratory, CNRS, to do programming support on supercalculators.